Finding Galaxy Groups in the Fields of Lensed Quasars

Catherine Grant & Mark Bautz (MIT Kavli Institute for Astrophysics and Space Research)

Abstract

Gravitationally lensed quasars can be used as an invaluable cosmological tool, however lens models often require a strong external shear in addition to the intrinsic eccentricity of the lensing galaxy to produce the observed asymmetry in the lensed images. The shear may be from a galaxy cluster or group associated with the lensing galaxy or otherwise along the line-of-sight to the quasar. We are searching for X-ray emission from groups and clusters in the fields of strong gravitational lenses using Chandra's resolving power to separate the bright quasar images from the much fainter diffuse emission. We present Chandra images and luminosities or luminosity limits for optically detected lensing groups associated with multiply imaged gravitationally lensed quasars. We also will discuss our search for extended X-ray emission in the fields of lensed quasars that are not yet known to contain a galaxy group.

Introduction

Gravitational lenses that produce multiple images of background quasars can be an invaluable tool for measuring cosmological parameters, to better study the magnified distant quasars, and to explore the structure of the lensing galaxies. Models require knowledge of the gravitational potential along the line of sight to the quasar including the lensing galaxy and any additional structure. Keeton et al. (2000) predict that a quarter of lensing galaxies are associated with a group or cluster that would perturb the gravitational potential. There are a handful of spectroscopically confirmed group- or cluster-lens associations and a number of intriguing photometrically identified galaxy overdensities. In addition there are many lensing systems that require additional shear components in order for models to reproduce the positions and fluxes of the quasar images. Among other possibilities, this additional shear could be due to a galaxy or cluster associated with the lensing galaxy or otherwise along the line of sight.

Groups or clusters have been previously studied in the X-ray in five of these systems including RX J0911+0551 (Morgan et al. 2001), Q0957+561 (Chartas et al. 1998), HST 14113+5211 (3C 295), and PG 1115+080 and B1422+231 (Grant et al. 2004). We are searching for X-ray emission from groups and clusters in the fields of strong gravitational lenses using Chandra's resolving power to separate the quasar images from diffuse emission. We have selected thirty multiply imaged quasars that are considered to be good lensing candidates and that have observations in the Chandra public archive. The previously studied groups are included in our sample to provide a useful comparison for the remaining targets.

Data Preparation

The thirty gravitational lenses were observed in fifty observations with a large range in exposure times and in a variety of configurations. The lenses were primarily observed using ACIS-S3 in standard full frame mode, however a few used the ACIS I-array, a sub-array or had the HETG inserted. Exposure times range from 5 to 198 ksec. The data were reduced using standard CIAO tools, including filtering by event grade and status and removing time periods with strong background flaring. Multiple observations of the same source were merged into a single event file. To maximize the diffuse signal and minimize the background, the event lists were filtered to include only photon energies between 0.5 and 2 keV, where the relative contribution of the particle background for the ACIS-S3 detector is at its lowest.

Image Analysis

Disentangling the much weaker extended emission from the bright quasar images is a complex task. Source detection detection algorithms such as `wavdetect` and `vtpdetect` are effective in finding isolated extended objects, but are less useful at differentiating nearly cospatial point sources and diffuse structures. To better remove the spatial distribution of the quasar emission, a model was constructed for the lens, with positions fixed to those measured in the optical and radio, and fit to the data in Sherpa. This lens model was then subtracted from the original image. Any remaining point sources in the image were excised and filled in using `dmfilth`. The images were then smoothed with a 30 pixel FWHM Gaussian and normalized for exposure variations and instrumental features.

Results

The quasar-subtracted, smoothed images were then examined to search for diffuse emission. Regions within four arcminutes of the lens and higher than 5-σ above the background level are considered detections. Twelve targets have detectable diffuse emission by this criteria including the five previously known X-ray sources. For the fields with detected extended emission, we list both the observed 0.5 - 2 keV flux and the bolometric X-ray luminosity for the region defined by the lowest contour level. The emission was assumed to be a Raymond-Smith plasma with Galactic absorption, a temperature of 1 keV and 0.3 solar abundances. The emission was assumed to be at the redshift of any previously known galaxy group or cluster, or at the redshift of the lensing galaxy. In some cases this implies multiple estimates for the multiple groups known to exist in the field. For the remaining eighteen lenses where we do not detect significant extended emission, we calculated the 3-sigma upper limits on the flux and luminosity.

Known X-ray Sources

Name	z_s	z_l	z_g	F_X (0.5-2 keV) (ph/cm^2/s)	L_{bol} (ergs/s)
RXJ0911+0551	2.80	0.77	0.77	$(1.04 \pm 0.07) \times 10^{-5}$	$(2.8 \pm 0.2) \times 10^{44}$
Q0957+561	1.41	0.36	0.36	$(1.07 \pm 0.06) \times 10^{-5}$	$(2.1 \pm 0.1) \times 10^{43}$
PG1115+080	1.72	0.31	0.31	$(2.2 \pm 0.3) \times 10^{-6}$	$(3.2 \pm 0.5) \times 10^{42}$
HST14113+5211	2.81	0.46	0.46	$(3.07 \pm 0.03) \times 10^{-4}$	$(1.30 \pm 0.01) \times 10^{45}$
B1422+231	3.62	0.34	0.34	$(3.5 \pm 0.3) \times 10^{-6}$	$(6.6 \pm 0.5) \times 10^{42}$

X-ray Upper Limits

Name	z_s	z_l	z_g	F_X (0.5-2 keV) (ph/cm^2/s)	L_{bol} (ergs/s)
Q0142-100	2.72	0.49	···	$< 2 \times 10^{-6}$	$< 1 \times 10^{43}$
HE0230-2130	2.16	···	···	$< 2 \times 10^{-6}$	$< 2 \times 10^{44}$
J0332-2756	···	0.62	···	$< 7 \times 10^{-7}$	$< 8 \times 10^{42}$
MG0414+0534	2.64	0.96	···	$< 1 \times 10^{-6}$	$< 1 \times 10^{44}$
HS0818+2554	3.12	0.39	···	$< 1 \times 10^{-6}$	$< 4 \times 10^{42}$
APM08279+5255	3.87	···	···	$< 1 \times 10^{-6}$	$< 1 \times 10^{44}$
BRI0952-0115	4.50	0.41p	···	$< 2 \times 10^{-6}$	$< 5 \times 10^{42}$
J1004+1229	2.65	0.95	···	$< 3 \times 10^{-6}$	$< 2 \times 10^{44}$
FSC10214+4724	2.29	0.75p	···	$< 2 \times 10^{-6}$	$< 3 \times 10^{43}$
HE1104-1805	2.32	0.73	···	$< 2 \times 10^{-6}$	$< 4 \times 10^{43}$
			2.0p		$< 5 \times 10^{45}$
H1413+117	2.55	0.9p	0.9p	$< 2 \times 10^{-6}$	$< 1 \times 10^{44}$
			1.7p		$< 2 \times 10^{45}$
HST14176+5226	3.40	0.81	···	$< 9 \times 10^{-7}$	$< 3 \times 10^{43}$
SBS1520+530	1.86	0.72	0.7p	$< 2 \times 10^{-6}$	$< 4 \times 10^{43}$
B1600+434	1.59	0.41	···	$< 1 \times 10^{-6}$	$< 4 \times 10^{42}$
B1608+656	1.39	0.63	0.63	$< 1 \times 10^{-6}$	$< 2 \times 10^{43}$
			0.26		$< 1 \times 10^{42}$
			0.43		$< 5 \times 10^{42}$
			0.52		$< 1 \times 10^{43}$
PKS1830-211	2.51	0.89	···	$< 1 \times 10^{-5}$	$< 1 \times 10^{45}$
MG2016+112	3.27	1.01	1.01	$< 2 \times 10^{-6}$	$< 4 \times 10^{44}$
Q2237+030	1.69	0.04	···	$< 1 \times 10^{-6}$	$< 2 \times 10^{40}$

Possible New X-ray Detections

Name	z_s	z_l	z_g	F_X (0.5-2 keV) (ph/cm^2/s)	L_{bol} (ergs/s)
B0712+472	1.34	0.41	0.29	$(3.8 \pm 0.9) \times 10^{-7}$	$(6 \pm 1) \times 10^{41}$
HS0810+2554	1.50	···	0.08	$(5.4 \pm 0.4) \times 10^{-5}$	$(2.9 \pm 0.2) \times 10^{42}$
LBQS1009-0252	2.74	0.88p	···	$(1.0 \pm 0.5) \times 10^{-6}$	$(5 \pm 2) \times 10^{43}$
Q1017-207	2.55	0.78p	···	$(3.7 \pm 0.7) \times 10^{-6}$	$(1.2 \pm 0.3) \times 10^{44}$
RXJ1131-1231	0.66	0.30	···	$(6 \pm 1) \times 10^{-6}$	$(8 \pm 1) \times 10^{42}$
MG1131+0456	···	0.84	0.84p	$(3.2 \pm 0.6) \times 10^{-6}$	$(6 \pm 1) \times 10^{42}$
			0.34		$(1.2 \pm 0.2) \times 10^{44}$
HE2149-2745	2.03	0.50	0.7p	$(2.5 \pm 0.7) \times 10^{-6}$	$(4 \pm 1) \times 10^{43}$

Contour Plots

The quasar-subtracted, smoothed images of the possible new X-ray detections are shown as contour plots. The lowest contour level is 3-σ above the background level and the contours are spaced by 2-σ. In the case of HS0810+2554 where the detection is highly significant, the contours are spaced by 10-σ. The blue diamonds are the lensed quasar images. The filled red triangles indicate spectroscopically confirmed galaxies in the group or cluster while the open red triangles are photometrically selected galaxies in the group or cluster. The green squares are the location of photometrically determined galaxy overdensities. North is up and east is to the left.

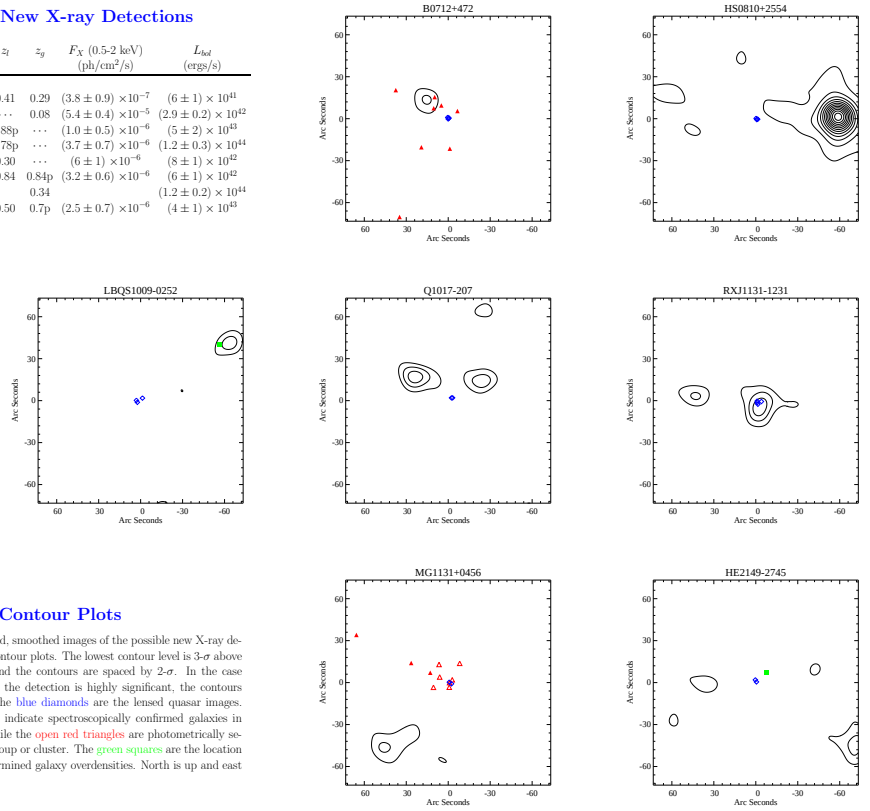

Discussion

We have discovered possible new diffuse X-ray emission towards seven of our targets. These span a wide range in luminosity and may, if real, represent both groups and clusters along the line of sight to these lenses. The most significant of these, towards HS0810+2554, is coincident with a galaxy in the 2MASS and SDSS catalogs. It was not detected in the RASS and has not been observed by any other X-ray mission. Examining the original event list, the emission is peaked at the galaxy location but is clearly diffuse, so may represent a hot galactic halo or a small galaxy group. Two of the targets, B0712+472 and LBQS1009-0252, have extended emission that is roughly coincident with known or suspected galaxy groups. The emission towards RXJ1131-1231 is roughly coincident with the lensing galaxy which may be a part of a small group. The nature of the emission in the remaining three targets, Q1017-207, MG1131+0456, and HE2149-2745, is not clear.

We observed thirty lensed quasars and detected extended emission in twelve or 40%. While it is possible that a few of our weaker detections are false, due to poor subtraction of point sources or understanding of the background distribution, it seems unlikely that they all are. In addition, for the fields in which no signficant extended source was found, the upper limits are often uninteresting and do not place strong constraints on the existence of a group or cluster. The incidence of groups and clusters in our sample seems to be higher than the Keeton et al (2000) estimate of 25%. Our sample is biased, however, due to the fact that lenses with larger separations that can be resolved by Chandra are more likely to be observed.

We plan to further refine our flux and luminosity measurements, in particular by using temperatures more appropriate to the known characteristics of the optically measured groups. We also intend to explore other smoothing algorithms, such as `csmooth`, to help confirm that our detections are real and not artifacts.

References

Chartas et al. 1998, ApJ, 504, 661
Grant et al. 2004, ApJ, 610, 686
Keeton et al. 2000, ApJ, 545, 129
Morgan et al. 2001, ApJ, 555, 1

Acknowledgments

The gravitational lens information was obtained from the CfA-Arizona Space Telescope Lens Survey (CASTLES) website (http://cfa-www.harvard.edu/castles) maintained by C. S. Kochanek, E. E. Falco, C. Impey, B. McLeod, H.-W. Rix. This research was supported by NASA contracts NAS-8-38252 and NAS-8-37716